Available online at www.sciencedirect.com
SCIENCE DIRECT
Journal of Organometallic Chemistry 691 (2006) 687–692
Journal of Organometallic Chemistry
www.elsevier.com/locate/jorganchem

Methyl abstraction kinetics of $CpFe(CO)_2Me$ using the benzyl radical clock

Thiam Seong Chong, Tsz Sian Chwee, Weng Kee Leong, Ming Wah Wong, Wai Yip Fan *

Department of Chemistry, National University of Singapore, 3 Science Drive 3, Singapore 117543, Singapore

Received 23 August 2005; accepted 3 October 2005
Available online 18 November 2005

Abstract

The rate constant for the methyl abstraction reaction of $CpFe(CO)_2Me$ has been measured with the benzyl radical clock as $(1.1 \pm 0.2) \times 10^5\ M^{-1}\ s^{-1}$ at room temperature. Time-resolved Fourier-transform Infrared (FTIR) absorption spectroscopy pointed towards the formation of the $CpFe(CO)_2$ radical upon benzyl abstraction. The main stable product has been established by a linear scan of the reaction mixture as $Cp_2Fe_2(CO)_4$ produced by the dimerization of the $CpFe(CO)_2$ radicals. The transition state structure for the abstraction process was also found at UB3LYP/6-311+G* level of theory to contain a planar CH_3 group.

Keywords: Methyl abstraction; Radical clock; IR spectroscopy

1. Introduction

Transition metal alkyl species continue to be widely employed in many chemical systems such as Fisher–Tropsch, alkene hydrogenation and hydroformylation catalytic process ever since their first systematic syntheses were accomplished fifty years ago [1–5]. Fundamental studies on the metal–carbon and metal–hydrogen bond strengths have been performed as well [6]. However by far the most important reaction involving the metal–carbon bond can be found in biological alkyl transfer reactions involving vitamin B12 and its derivatives [7,8]. For example, the methyl transfer from an organocobalt(III) to nickel(I) species was investigated recently as this process serves as a model for acetyl coenzyme A synthesis [9]. Methyl transfer reaction rate coefficients to organometallic nucleophiles such as $Fe(CO)_4^{2-}$ and $CpFe(CO)_2^-$ have also been observed for several transition metal carbonyl species using an infrared stopped-flow spectrometer [10,11]. Hence, quantitative measurements of the transfer or abstraction rates of transition metal alkyl species are vital for gaining a better understanding of such reaction mechanistic studies.

Measurements of hydrogen atom abstraction rates in organometallic hydride species have been performed using radical clock methods [12–14]. Recently the benzyl radical, $PhCH_2$, has been utilised as a radical clock; it can either abstract a hydrogen atom from an organometallic hydride to form toluene, or undergo self-recombination to form bibenzyl [15]. Franz et al. [15,16] have successfully applied this radical clock to measure the abstraction rate of hydrogen atom from $Cp^*Mo(CO)_3H$ and triosmium clusters.

However radical clocks have not been used for alkyl abstraction rates. Herein, we would like to report our study using $CpFe(CO)_2Me$ as an example to demonstrate the possibility of extending benzyl radical clock kinetics to methyl transfer processes. We chose $CpFe(CO)_2Me$ for several reasons; it is commercially available, relatively less air-sensitive than most metal-alkyls and its abstraction process may be followed by both linear-scan and time-resolved IR spectroscopy via its carbonyl stretches. In this way, we hope to obtain evidence as to whether the abstraction proceeds via a neutral radical or an ionic pathway. Since this is the first use of radical clocks to methyl abstraction, it is

* Corresponding author. Tel.: +65 68746823/96385110; fax: +65 67791691.
E-mail address: chmfanwy@nus.edu.sg (W.Y. Fan).

0022-328X/$ - see front matter © 2005 Elsevier B.V. All rights reserved.
doi:10.1016/j.jorganchem.2005.10.010

important to gain a detail understanding of the process before the method could be applied to more important systems such as the cobalt–carbon bond cleavage in vitamin B12 derivatives. In our experiment, a xenon lamp was used to photodissociate the 1,3-diphenyl-2-propanone (dibenzylketone, DBK) precursor to form the benzyl radical. Gas chromatography was then used to determine the relative concentrations of the organic products derived from the abstraction process, from which the rate constant of methyl transfer from $CpFe(CO)_2Me$ to the benzyl radical could be inferred. The kinetics of the reactive intermediates and stable products of the reaction were also monitored using both time-resolved and linear scan FTIR spectroscopies. Density functional methods in GAUSSIAN 98 were used to determine the energetics and transition state structure of the methyl abstraction reaction.

2. Experiment

Toluene, bibenzyl, ethylbenzene, *t*-butylbenzene and hexane were purchased from Sigma–Aldrich and dried and degassed prior to use. Dibenzylketone (98%) was purified by several recrystallizations from hexane. $CpFe(CO)_2Me$ was obtained from Sigma–Aldrich and used as received. An osmium hydride cluster species $Os_3(\mu\text{-}H)(H)(CO)_{10}(PPh_3)$, to be used as a clock standard, was synthesised according to the literature method, [17]. Generally, all the sample manipulations were carried out under N_2 environment. About 2–10 mg of the organometallic carbonyl species ($\approx 10^{-4}$ M), 8–15 ml DBK (10^{-4}–10^{-3} M) and 20 ml hexane as solvent were added into a round-bottomed flask. Oxygen-free nitrogen gas was used to deoxygenate the solution before photolysis was initiated.

A broadband xenon lamp (200 W, 300–700 nm) was used for the photodissociation of DBK. The reaction mixture was irradiated for 5–20 min before sampling of the products for GC analysis. The output of the lamp energy was monitored by placing a fiber optic cable close to the reaction vessel so that some light was directed into an Acton research monochromator (focal length 30 cm). The intensity of the light was monitored over a broad range of wavelengths (300–500 nm) during the irradiation process to ensure constancy of output. An infrared filter was placed in front of the lamp in order to minimise any increase in temperature; hence during irradiation, the temperature could be maintained at 25.5 ± 0.5 °C read by a thermocouple attached onto the wall of the flask.

Gas chromatography (GC) analysis was carried out on a Hewlett–Packard 5890 Series II equipped with a splitless injector, capillary column and a flame-ionization detector. GC analysis of unphotolyzed samples was performed prior to each kinetic run to establish the background concentrations of toluene, ethylbenzene and bibenzyl. For standardization, a stock solution which is 1.00×10^{-4} M each in toluene, bibenzyl, ethylbenzene and *t*-butylbenzene in hexane was further diluted with a stock solution of 1.00×10^{-4} M *t*-butylbenzene in hexane, to concentration ranges between 5.00×10^{-7} and 5.00×10^{-5} M. Plots of GC peak area ratios (analyte/*t*-butyl benzene) versus molarity ratios (analyte/*t*-butylbenzene) yielded linear plots over this concentration range. A series of three experiments conducted with different concentration ratios of $CpFe(CO)_2CH_3$ (2×10^{-4} M) and DBK (4, 8 and 12×10^{-4} M) and at each 10 min interval for a total of 30 min of irradiation, the reaction mixture was sampled and the products analysed by GC.

A brief description of the cell used for performing linear and time-resolved FTIR spectroscopy on the reaction mixture is given here. It is a stainless steel, static, liquid cell with CaF_2 windows for passage of the IR probe beam. Absorbance path-lengths of 0.5–5 mm could be accommodated by manual adjustment of the window holders. The cell also allowed for placement of quartz or glass windows to permit photodissociation by a laser beam propagated at right angles to the IR probe beam. The cell could hold a volume of about 40 ml of solvent, together with a magnetic bar to provide constant stirring. Inlet and outlet ports on each side of the cell allowed for N_2 bubbling through the solution if required.

For the detection of intermediates and stable products of the reaction, a frequency-tripled Nd-YAG pulsed-laser (Continuum Surelite III-10, 355 nm, 10 Hz, 20 mJ/pulse) was used as the photodissociation source. The laser beam was focused by a cylindrical lens into an elliptical spot (about 5 mm × 0.2 mm). A significant overlap with the FTIR beam propagated at right angles to the laser beam could be achieved this way, optimising the sensitivity for radical detection. The infrared range and resolution of the Nicolet Nexus 870 FTIR spectrometer were set at 1000–4000 and 2–4 cm^{-1}, respectively. Linear scan FTIR spectra were taken at intervals of 5 min after initiation of photolysis, with averaging over 16 scans each time. For the time-resolved experiments, a digital delay generator (Stanford Research Digital Delay Generator DG 535) was employed to achieve synchronization of the FTIR spectrometer with the firing of the pulsed laser. An AC-coupled detector (TRS-20 MHz HgCdTe) attached with a Ge window (for shielding the detector from stray light) was used so that only changes in the IR absorption in steps of 1 μs would be captured. We have found that only one complete scan of the spectrum, which lasted about 30 min, was sufficient to produce detectable signals of the radicals.

The reaction profile for methyl abstraction from $CpFe(CO)_2Me$ by benzyl radical was studied using the hybrid B3LYP [18,19] density functional method together with the triple-split valence polarized 6-311+G* basis set. Spin-restricted calculations were used for closed-shell systems and spin-unrestricted ones (i.e., UB3LYP) for open-shell species. The structures of the reactants ($CpFe(CO)_2Me$ and benzyl radical), products ($CpFe(CO)_2^{\cdot}$ and ethylbenzene), and transition state for methyl transfer were fully optimized at the B3LYP/6-311+G* level. Harmonic frequencies were calculated at the optimized geometries to

characterize stationary points as equilibrium structures, with all real frequencies, or transition states, with one imaginary frequency, and to evaluate zero-point energy (ZPE) correction. The free energy of activation ($\Delta G^{\neq}$) were computed from the equation $\Delta G_T^{\neq} = \Delta H_T^{\neq} - T\Delta S^{\neq}$, where $\Delta S^{\neq}$ is the entropy change and $\Delta H_T^{\neq} = \Delta H_0^{\neq} + (H_T^{\neq} - H_0^{\neq})$. The computed vibrational frequencies and ZPE were scaled by 0.96 and 0.98, respectively [20]. All calculations were performed using the GAUSSIAN 98 suite of program [21].

3. Results and discussion

The derivation of the rate constant for the benzyl abstraction from an organometallic species was reported previously for $CpMo(CO)_3H$ and subsequently used for the osmium hydride cluster work as well [15,16]. The photolysis of DBK provides a readily accessible source of benzyl radicals. Rate constants were determined in competitive kinetic experiments that measured the rate of formation of toluene from benzyl radicals in competition with self-termination of benzyl radicals to form bibenzyl [2,3]. Under a constant rate of photolysis of DBK and low conversion of the hydrogen atom donor, the relationship between toluene, bibenzyl and the hydrogen donor concentration over a period of photolysis, Δt (in seconds), is

$$k_{abs(H)} = \{[\text{toluene}]k_t^{1/2}\}/\{[\text{bibenzyl}]^{1/2}[\text{M–H}]\Delta t^{1/2}\}. \quad (1)$$

We have also used this expression for determining the abstraction rate of $Os_3(\mu\text{-H})(H)(CO)_{10}(PPh_3)$ and obtained $k_{Abs(H)} = 7.7 \times 10^{-4}\ M^{-1}\ s^{-1}$ at 298 K. This value is in very good agreement with the value of $8.2 \times 10^{-4}\ M^{-1}\ s^{-1}$ previously determined under similar conditions and hence demonstrated the reproducibility of the results and the suitability of our experimental conditions to conduct further radical clock reactions.

For the methyl abstraction case, modifications to the equation are required where $k_{abs(H)}$, [toluene] and [M–H] are replaced by $k_{abs(H)} = k_{abs(Me)}$, [ethylbenzene] and [M–CH_3], respectively, to yield

$$k_{abs(Me)} = \{[\text{ethylbenzene}]k_t^{1/2}\}/\{[\text{bibenzyl}]^{1/2}[\text{M–CH}_3]\Delta t^{1/2}\}. \quad (2)$$

We found that the increase in the concentration of bibenzyl and ethylbenzene were linear over 20 min of photolysis in a series of three experiments conducted with different concentrations of $CpFe(CO)_2CH_3$ and DBK. A minute amount of toluene was detected by GC (<3% of ethylbenzene) and hence its contribution was neglected for the calculations. The low level of toluene was not surprising since hydrogen abstraction from a strong C–H bond in DBK should be much more difficult than methyl abstraction from a much weaker metal–carbon bond of an organometallic species. A high toluene concentration would have indicated that hydrogen atom abstraction from DBK competed with the methyl abstraction from $CpFe(CO)_2Me$ and this additional pathway would have to be taken into account in the calculations. However, our observations lend support to the use of the simple formula above for the estimation of the methyl abstraction rate. We have found that over the period of irradiation for GC analysis, the concentration of $CpFe(CO)_2Me$ did not change by not more than 5%. As Eq. (2) demands that [M–CH_3] stays roughly constant, we take the concentration to be the average between the initial and the final concentration reading over the photolysis time.

As a control experiment, $CpFe(CO)_2Me$ itself was also photolysed over the same irradiation time in the absence of DBK but no products were observed although decarbonylation of the compound may have taken place. We have also attempted to detect methane and ethane gases that might be released if the methyl group were to dissociate upon photolysis. However, even after two hours of photolysis, the IR spectrum did not show any vibrational bands due to these two species. Hence the results here show that ethylbenzene was mainly produced by benzyl radical abstraction of $CpFe(CO)_2Me$ rather than through photodecomposition of the latter.

The measured average abstraction rate constant, $k_{abs(CH_3)}$ was $(1.1 \pm 0.2) \times 10^5\ M^{-1}\ s^{-1}$, after substituting the appropriate value for the bibenzyl formation rate constant [15]. To our knowledge, this is the first reported quantitative measurement of a methyl transfer reaction from an organometallic species using a radical clock. One can perhaps compare this value with various determinations of hydrogen atom or methyl transfers, but such comparisons are difficult. A brief summary of the relevant work is given here instead. For example, the previously measured hydrogen atom abstraction rate from $CpFe(CO)_2H$ by the α-cyclopropylstyrene radical clock system was as high as $10^9\ 4\ M^{-1}\ s^{-1}$ [13,14]. On the other hand, the same hydrogen atom transfer rate determined with the trityl radical clock was much slower, at $1.2 \times 10^4\ M^{-1}\ s^{-1}$ [22]. Thus the measured transfer rates are influenced by steric factors as well as by bond energies, and are a function of the radical clock employed. Furthermore, hydrogen atom abstraction rates for different organometallic hydride species can vary over a wide range; values from 1 to $10^9\ M^{-1}\ s^{-1}$ have been reported. Unfortunately, the benzyl radical clock has not been used on $CpFe(CO)_2H$ yet hence precluding a direct comparison between the methyl abstraction rate of $CpFe(CO)_2Me$ and the hydrogen atom abstraction of $CpFe(CO)_2H$. We have attempted to synthesize $CpFe(CO)_2H$ but several attempts failed because of the air-sensitivity of the species. Methyl transfer rates to $Fe(CO)_4^{2-}$ and $CpFe(CO)_2^-$ anions have also been measured previously with various transition metal carbonyl species [10,11].

Scheme 1 shows the possible reactions for the methyl abstraction of $CpFe(CO)_2Me$ by the benzyl radical.

As mentioned, we have attempted to understand the abstraction pathway by monitoring the evolution of reactants, products and reactive intermediates using FTIR spectroscopy. The methyl abstraction process was followed

(1) $PhCH_2COCH_2Ph\ (+h\nu) \rightarrow 2\,PhCH_2 + CO$

(2) $PhCH_2 + PhCH_2 \rightarrow$ bibenzyl

(3) $PhCH_2 + CpFe(CO)_2Me \rightarrow$ ethylbenzene + $CpFe(CO)_2$

(4) $PhCH_2 + PhCH_2COCH_2Ph \rightarrow$ toluene + products

(5) $2CpFe(CO)_2 \rightarrow Cp_2Fe_2(CO)_4$

(6) $PhCH_2 + CpFe(CO)_2 \rightarrow CpFe(CO)_2CH_2Ph$

(7) $CpFe(CO)_2Me\ (+h\nu) \rightarrow$ products

Scheme 1.

by linear-scan FTIR spectroscopy to record the gradual decay of the precursor and the formation of stable products. Fig. 1 shows that by far the dominant organometallic product formed during the course of the reaction over 2 h was the dimeric $[CpFe(CO)_2]_2$ ($\nu_{CO} = 1800$, 1960 and 1995 cm^{-1} in hexane) in accordance to the above reaction scheme [23]. Upon abstraction of the methyl radical from $CpFe(CO)_2Me$, the $CpFe(CO)_2$ radical formed will dimerise quickly. We did not observe the $CpFe(CO)_2CH_2Ph$ product although its carbonyl stretches in the infrared spectrum lie very close to the $CpFe(CO)_2Me$ bands [24]. Nevertheless it should still be possible to observe a shoulder or broadening of the $CpFe(CO)_2Me$ bands due to the appearance of $CpFe(CO)_2CH_2Ph$. However, these features were not observed throughout two hours of photolysis during a linear FTIR scan of the reaction. Hence this would suggest that either reaction 6 is slow or that once this species is formed, it immediately reacts with the benzyl radical to form bibenzyl and $CpFe(CO)_2$. The increased concentration of bibenzyl due to this additional reaction might have caused the methyl transfer rate coefficient to be slightly underestimated.

A time-resolved FTIR spectrum was recorded during the initial stages of irradiation and a small signal due to the $CpFe(CO)_2$ radical at 1938 cm^{-1} was detected [23]. Since the signal-to-noise ratio was low, the chemical lifetime of the radical could only be estimated to be approximately 6 μs by monitoring the time for its IR signal to disappear into the noise level. We have also been unable to record the weaker carbonyl band of the radical at 2004 cm^{-1} because of the low S/N ratio. However, the signal at 1938 cm^{-1} was reproducible over many different runs of the reaction. The fact that the TRS spectrum showed only a weak radical signal at 1938 cm^{-1} was attributed to the use of low laser energy to irradiate the reaction mixture. Since a low yield of benzyl radical from 355 nm photolysis of DBK is expected because of its small absorbance, the concentration of the $CpFe(CO)_2$ is also expected to be small (see Fig. 2).

Control experiments in which either $CpFe(CO)_2Me$ or DBK was absent did not show this signal. Although $[CpFe(CO)_2]_2$ also photodissociates at 355 nm to yield two $CpFe(CO)_2$ radicals, we believe that most of the radicals originated from the benzyl abstraction of $CpFe(CO)_2Me$; since the TRS spectrum was taken at the first twenty minutes of photoirradiation, there was hardly any time for the dimer contribution to build up and contribute significantly to the radical concentration. That only a very small amount of the dimer was formed during the first twenty minutes of the reaction was confirmed by a linear FTIR scan. However a very weak TRS signal of

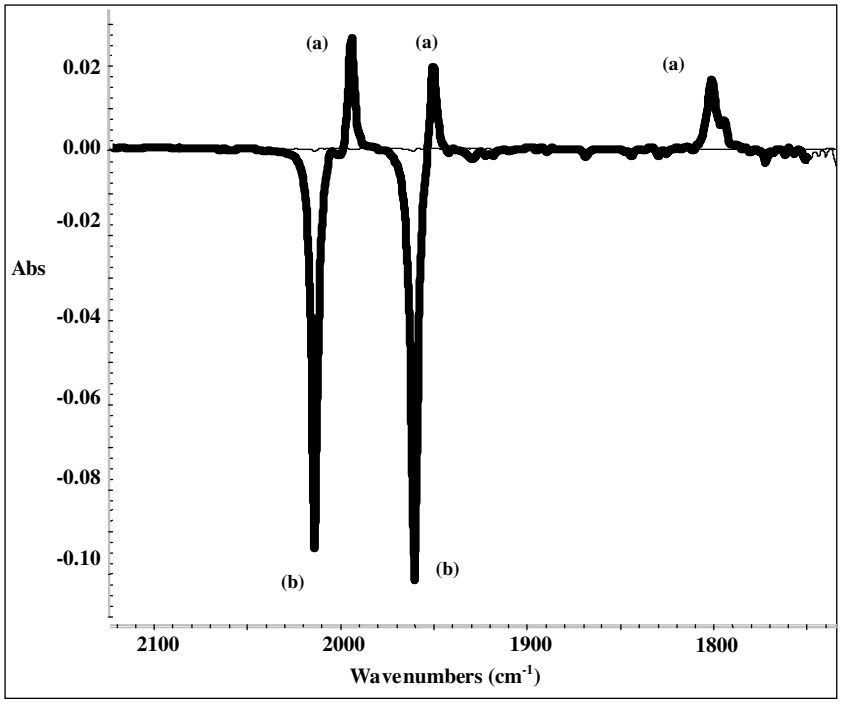

Fig. 1. The production of $Cp_2Fe_2(CO)_4$ (label a) after 2 h of 355 nm photolysis of DBK in the presence of $CpFe(CO)_2Me$ (label b).

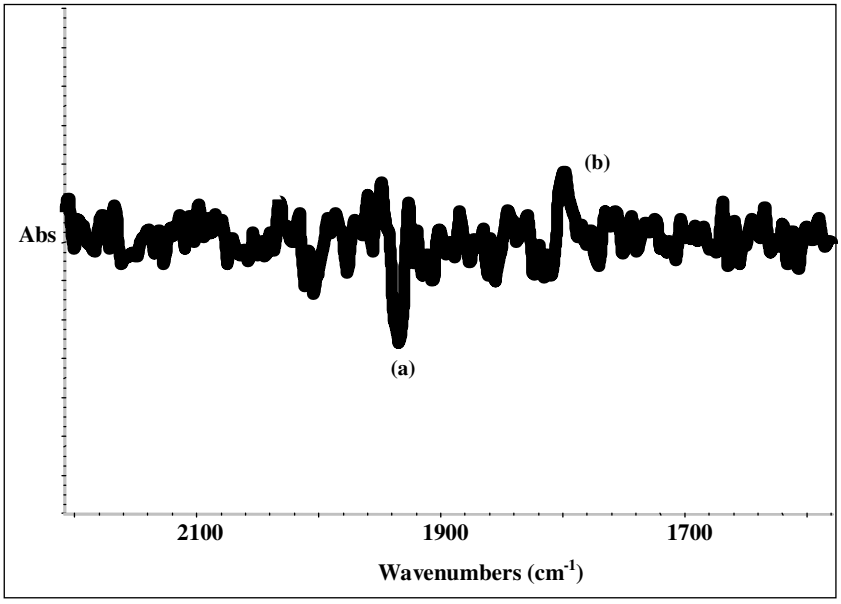

Fig. 2. A time-resolved FTIR spectrum showing the production of $CpFe(CO)_2$ radical (label a) from the 355 nm photolysis (15 mJ/pulse) of $CpFe(CO)_2Me$ recorded 10 μs after initiation of photolysis. Only the stronger of the two IR bands at 1938 cm^{-1} could be observed. The spectrum here was recorded at 5 μs after the laser initiation pulse.

$CpFe(CO)_2$ dimer could be seen as a peak at 1800 cm^{-1} pointing in the opposite direction to the radical signal. This is not surprising since the TRS technique is well-known to be able to capture reversible changes of intermediate species such as the $CpFe(CO)_2$ dimer undergoing metal–metal bond photodissociation and formation in solution. In the case of the $CpFe(CO)_2Me$ precursor, its TRS signal could not be captured simply because it decays in a irreversible manner once the methyl group has been abstracted.

We have also determined that the laser energy was not intense enough to induce multiphoton dissociation process by monitoring the evolution of the bibenzyl and ethylbenzene products in the same way as with the broadband irradiation. In one experiment, two flasks of the reaction mixture of the same composition were each photolysed by the laser and the xenon lamp for the same duration, respectively. GC analysis of the products showed that the ethylbenzene and bibenzyl signals upon laser photolysis at the same energy used to generate the TRS spectrum, were only about 10% higher compared to broadband irradiation. This comparison lends confidence to the fact that the laser power used did not induce different and significant effects, at least on the reactions pathway of product formation.

We have not observed any methyl migration of $CpFe(CO)_2Me$ upon photolysis. This is perhaps not surprising since the 16-electron intermediate formed after any methyl migration is not expected to be stable in the absence of excess CO. It therefore appears that a simple methyl abstraction process takes place for the benzyl radical abstraction of $CpFe(CO)_2Me$. Reactions 1, 2, 3 and 5 are thus the dominant pathways while reactions 4, 6 and 7 are either minor or absent.

The reaction profile for methyl abstraction from $CpFe(CO)_2Me$ by benzyl radical was studied theoretically by the B3LYP/6-311+G* level of theory. The optimized geometry of the transition state is shown in Fig. 3. As with most radical abstraction reactions, the Fe···CH_3···C framework in the transition state is almost linear (175.2°). The Fe···C breaking bond (2.351 Å) is 14% lengthened compared to that in $CpFe(CO)_2Me$ (2.056 Å). On the other hand, the C···C forming bond (2.309 Å) is substantially longer than the C–C bond in ethylbenzene (1.538 Å). This clearly indicates that the transition state structure is reactant-like and corresponds to an early transition state. This is readily expected according to Hammond's postulate for an exothermic reaction. It is interesting to note that the methyl group in the transition state adopts a planar geometry (as

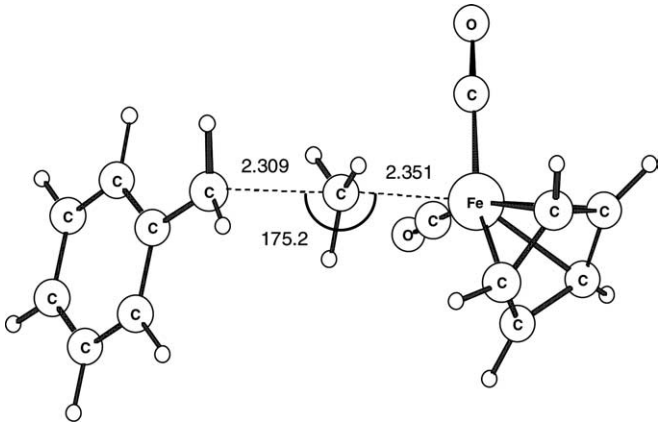

Fig. 3. Optimized (B3LYP/6-311+G*) transition state geometry for the methyl abstraction reaction of $CpFe(CO)_2Me$ by benzyl radical, bond lengths in (Å) and angles in (°).

indicated by the near 120° angles), which corresponds to the structure of a methyl radical. Indeed, calculation indicates that the spin densities are localized mainly in the Fe atom, methyl carbon and methylene carbon of the benzyl moiety in the Fe···CH_3···C framework.

The geometries of the $CpFe(CO)_2$ and benzyl moieties are effectively unchanged in the transition state compared to the reactants. It is worth noting that the geometry of product $CpFe(CO)_2^{\bullet}$ radical is virtually the same as the reactant $CpFe(CO)_2Me$, for instance, the CO–Fe–CO angles are 94.2° and 94.8°, respectively. This methyl abstraction reaction is predicted to be strongly exothermic, $\Delta E_0 = -155.1\ \mathrm{kJ\ mol^{-1}}$ and $\Delta G_{298} = -159.1\ \mathrm{kJ\ mol^{-1}}$. Accordingly, this methyl transfer process is inhibited by a small energy barrier, $\Delta E_0^{\neq} = 68.0\ \mathrm{kJ\ mol^{-1}}$ and $\Delta G_{298}^{\neq} = 108.0\ \mathrm{kJ\ mol^{-1}}$. A significantly greater magnitude of free energy of activation is attributed to the fact that the transition state is more ordered compared to the reactants (i.e., negative $\Delta S^{\neq}$). The calculated energetics of the methyl transfer process is in accord with the experimental finding.

In summary, we have shown that reaction of $CpFe(CO)_2Me$ by benzyl radical proceeds via simple methyl abstraction. A rate constant of $1.1 \times 10^5\ \mathrm{M^{-1}\ s^{-1}}$ at 298 K has been established using gas chromatography to record the relative concentrations of the ethylbenzene and bibenzyl products and a simple rate expression. Infrared spectroscopic evidence pointed towards the formation of the $CpFe(CO)_2$ radical which then undergoes dimerization. A transition state structure corresponding to the abstraction process was also found at the UB3LYP/6-311+G* level of theory in which the CH_3 group to be transferred adopts a planar geometry. Work is underway to measure the rate constants of phosphine and carbene derivatives of $CpFe(CO)_2Me$ in order to examine any stereoelectronic effects of such ligands.

Acknowledgements

This work was supported by the Agency of Science, Technology and Research (ASTAR) under Grant No. 012-101-0035. T.S.C. thanked the Institute of Chemical and Engineering Science (ICES) of Singapore for a research scholarship.

Appendix A. Supplementary data

Supplementary data associated with this article can be found, in the online version, at doi:10.1016/j.jorganchem.2005.10.010.

References

[1] T.S. Piper, G. Wilkinson, J. Inorg. Nucl. Chem. 3 (1956) 104.
[2] H. Tan, A. Yoshikawa, M.S. Gordon, J.H. Espenson, Organometallics 18 (1999) 4753.
[3] P.M. Maitlis, J. Organomet. Chem. 689 (2004) 4366.
[4] J.R. Moss, J. Mol. Catal. A 107 (1996) 169.
[5] A. Haynes, B.E. Mann, G.E. Morris, P.M. Maitlis, J. Am. Chem. Soc. 115 (1993) 4093.
[6] J.A. Labinger, J.E. Bercaw, Organometallics 7 (1988) 926.
[7] A.I. Scott, Pure Appl. Chem. 68 (1996) 2057.
[8] J.J. Shiang, L.A. Walker II, N.A. Anderson, A.G. Cole, R.J. Sension, J. Phys. Chem. B 103 (1999) 10532.
[9] M.S. Ram, C.G. Riordan, G.P.A. Yap, L. Liable-Sands, A.L. Rheingold, A. Marchaj, J.R. Norton, J. Am. Chem. Soc. 119 (1997) 1648.
[10] P. Wang, J.D. Atwood, J. Am. Chem. Soc. 114 (1992) 6424.
[11] P. Wang, J.D. Atwood, Organometallics 12 (1993) 4247.
[12] D. Griller, K.U. Ingold, Acc. Chem. Res. 13 (1980) 323.
[13] R.M. Bullock, E.G. Samsel, J. Am. Chem. Soc. 109 (1987) 6542.
[14] R.M. Bullock, E.G. Samsel, J. Am. Chem. Soc. 112 (1990) 6886.
[15] J.A. Franz, J.C. Linehan, J.C. Birnbaum, K.W. Hicks, M.S. Alnajjar, J. Am. Chem. Soc. 121 (1999) 9824.
[16] J.A. Franz, D.S. Kolwaite, J.C. Linehan, E. Rosenberg, Organometallics 23 (2004) 441.
[17] J.R. Shapley, J.R. Keister, M.R. Churchill, J. Am. Chem. Soc. 97 (1975) 4145.
[18] D.A. Becke, J. Chem. Phys. 98 (1993) 5648.
[19] C. Lee, W. Yang, R.G. Parr, Phys. Rev. B 37 (1988) 785.
[20] M.W. Wong, Chem. Phys. Lett. 256 (1996) 391.
[21] M.J. Frisch et al., GAUSSIAN 98, Gaussian Inc., Pittsburgh, PA, 1998.
[22] D.C. Eisenberg, C.J.C. Lawrie, A.E. Moody, J.R. Norton, J. Am. Chem. Soc. 113 (1991) 4888.
[23] A.J. Dixon, M.W. George, C. Hughes, M. Poliakoff, J.J. Turner, J. Am. Chem. Soc. 114 (1992) 1719.
[24] J.P. Blaha, M.S. Wrighton, J. Am. Chem. Soc. 107 (1985) 2694.